Acta Acustica united with Acustica
Vol. 98 (2012) 158 – 165

DOI 10.3813/AAA.918501

Wave Propagation and Radiation in a Horn: Comparisons Between Models and Measurements

P. Eveno[1)], J.-P. Dalmont[2)], R. Caussé[1)], J. Gilbert[2)]
[1)] Ircam (UMR CNRS 9912), 1 place Igor Stravinsky, 75004 Paris, France. pauline.eveno@ircam.fr
[2)] Laboratoire d'Acoustique de l'Université du Maine (UMR CNRS 6613), 72085 Le Mans, France

Summary
The modeling of wave propagation in a horn is still problematic as the limit of plane wave approximation is known but no method is proven to give accurate results. This paper proposes to evaluate the error induced by both a plane wave model and a spherical model. These models use a Transmission-Matrix Method based on either plane or quasi-spherical propagation and loaded with two different radiation impedances. This study is done on two musical instruments horns, one from a trumpet and the other from a trombone, whose geometry is known to within a tenth of millimetre. The respective influence of both propagation and radiation is observed by comparing the input impedance measured on each of the two horns with the impedance calculated with both models. Differences between models and measurements are quantified and an extension to a whole trombone is also done. The spherical model approximates the behaviour of the horn with an improved accuracy and differences between the model and the measurement do not rise above 25 cents.

PACS no. 43.20.Mv, 43.75Fg

1. Introduction

The input impedance of a wind instrument is a quantity that gives important informations regarding the instrument's playing behaviour [1, 2, 3, 4]. It can be either calculated or measured, in most cases with a sufficiently good accuracy, given that the human ear is able to detect frequency shifts of 0.2% (3 cents) [5]. Starting from the wind instrument shape, the Transmission-Matrix Method based on the plane wave approximation is usually considered as the most straightforward method of calculating the input impedance. Indeed, comparisons have shown that good correlation with measurements can be obtained [6, 7]. However, in the case of brass instruments, the modeling of the horn is still problematic as the plane wave approximation is no longer valid when the slope of the horn is too large. This limit is well known but to date no method is proven to give accurate results. The aim of the present article is to evaluate the error induced by the plane wave approximation and to check another Transmission-Matrix Method based on quasi-spherical wave propagation. The radiation impedance is also problematic as it is well known in the case of a cylinder but not in the case of a cone or a horn. An alternative radiation impedance proposed by [8] is also tested in the present paper. Results are compared with measurements, for which the accuracy in terms of the resonance frequencies is shown to be within 3 cents.

Section 2 presents the state of the art and theory of the propagation and radiation models that are used in this article. Section 3 describes the set-up used for the measurements as well as the horns studied. Then, results of computation and measurements are compared and discussed. Finally, as this work is part of a project aimed at helping craftsmen to design and characterize their musical instruments, an application for craftsmanship is presented in section 4 in the form of an entire computed trombone.

Received 8 June 2011,
accepted 26 October 2011.

2. Propagation and Radiation in a horn

2.1. Propagation models

The wind instrument air columns have been studied by scientists for a long time [9, 1]. One of the simplest and most efficient methods is the Transmission-Matrix Method (TMM). This method approximates the instrument structure as a sequence of concatenated segments, cylinders or cones, each being mathematically represented as a 2x2 matrix in which the terms are complex-valued and frequency-dependent. An extension of the TMM to modes -the Multimodal Method- can also be applied to that case (see for example Amir *et al.* [10] or the method reviewed by Kemp [11, 12]). Nevertheless, other methods have been used to analyse the air column, such as the Finite Element Method [13] and the Finite Difference Method [14]. Such

numerical methods, based on the discretization of the geometry in small elements for which fundamental equations can be solved, have the advantage that complex geometries, such as musical instruments, can be handled easily. However, the huge computation time necessary to solve a complete instrument model is a serious drawback for craftsmanship applications.

On the other hand, with an entire instrument described as a transmission line, it is easy to calculate quantities at the input end, defined as the usual point of excitation, given quantities at the output end.

The Transmission-Matrix Method used in this article is described in the article of Caussé *et al.* [15]. This method has been proven to give results close to measured values for wind instruments of cylindrical geometry when a plane wave approximation is used [6, 7]. However, for horns, it is not possible to assume plane wave propagation any more [16, 17]. This is why Nederveen and Dalmont [18] propose a low frequency correction for the TMM in the form of an additional impedance that takes into account the transverse flow inside the horn. Nevertheless, a problematic issue is that the wavefront is still unknown.

Another approach is that of Agulló *et al.* [19] who assume the time-invariance of equipotential surfaces normal to the profile and the axis of an axisymmetric horn and develop 1D models for both spherical and oblate ellipsoidal surfaces. Keefe and Barjau [20] use this model for a hyperbolic horn and find it to be more accurate than the plane-wave horn equation or the spherical-wave horn equation of Benade and Jansson [16, 17]. Nevertheless this method cannot be applied to an arbitrary horn geometry, especially for a rapidly changing horn profile. For such cases, Hélie [21] proposes a model with a geometrical hypothesis (quasi-sphericity of isobars near the wall) which does not require fixed wavefronts as usual. This hypothesis leads to a solution of the Webster equation with curvilinear abscissa.

For craftsmanship applications it is important to have a reliable resolution that works for all geometries. That is why it is preferable to use only truncated cones or cylinders, and apply them in a Transmission-Matrix Method. The horn equation with curvilinear abscissa derived in [21] for quasi-spherical isobars also corresponds to the continuous model obtained for piecewise conical segments when the length of cones uniformly tends towards zero. Moreover, the artefacts due to the choice of cones rather than a C^1 regular profile are negligible if the slope change between the cones is sufficiently small (see [22]). Hence, in this article, we choose to compute the TMM using piecewise conical segments obtained for a sufficiently refined mesh description. Then, we compare this piecewise spherical model with a plane model constructed from the TMM calculated along the horn axis.

2.2. Radiation models

The problem of the acoustic radiation impedance of a cylindrical pipe is now well known. Cases of unflanged and infinitely flanged cylinders have been solved [23, 24]. These results are extended by Silva *et al.* [25] above the cutoff frequency of the first higher order mode. They give a non-causal expression obtained by analytical and numerical fitting to reference results from Levine and Schwinger for the unflanged case and extracted from the radiation impedance matrix given by Zorumski [26] for the infinite flanged case. Furthermore, measurements on tubes with various flanges that can be found in musical instruments have been compared to theoretical and numerical results [27].

However, these radiation impedances cannot be used in every case. Indeed, the shape of a horn has a strong influence on the acoustic radiation, to such an extent that it is no longer justified to use a plane radiation impedance. This is why Caussé *et al.* [15] have introduced a correction for the case of spherical waves, normalizing the Levine's expression by the ratio A_p/A_s where A_p and A_s are respectively the planar and spherical wavefront areas. However, the large discrepancies betwee their model and the measurement of a trombone bell indicate the need for an improved model of the radiation impedance. To this end, Hélie and Rodet [8] then propose approximating the radiation of a horn by that of a pulsating portion of sphere, as was first calculated by [28, 29], and give analytical formulae.

This article aims at comparing two types of model: a plane wave model and a spherical wave model. An unflanged case seems to fit well with the geometry of a horn. The radiation impedance from Silva *et al.* [25] is thus chosen as the plane wave model to be used above the cutoff frequency.

The pressure reflection coefficient is defined as $R = -|R|e^{-2ikL}$.

Silva *et al.* give the modulus of the pressure reflection coefficient of an unflanged pipe as

$$|R(\omega)| = \frac{1 + a_1(ka)^2}{1 + (\beta + a_1)(ka)^2 + a_2(ka)^4 + a_3(ka)^6}, \qquad (1)$$

with $a_1 = 0.800$, $a_2 = 0.266$, $a_3 = 0.0263$ and $\beta = 1/2$. $k = \omega/c$ is the acoustic wavenumber and a is the cylinder radius (or the radius of the output end of the horn as shown in Figure 1). L is the end correction due to radiation and its expression is given by

$$\frac{L}{a} = \eta \frac{1 + b_1(ka)^2}{1 + b_2(ka)^2 + b_3(ka)^4 + b_4(ka)^6}, \qquad (2)$$

with $\eta = 0.6133$, $b_1 = 0.0599$, $b_2 = 0.238$, $b_3 = -0.0153$ and $b_4 = 0.00150$. The radiation impedance Z_r can be then expressed as

$$Z_r(\omega) = Z_c \frac{1 + R}{1 - R}, \qquad (3)$$

where $Z_c = \rho c/\pi a^2$ is the characteristic impedance.

With regard to a spherical model, Hélie and Rodet give an analytical solution for the radiation of a sphere, part of which is pulsating (see Figure 1) with a uniform velocity while the rest remains motionless, though it remains to

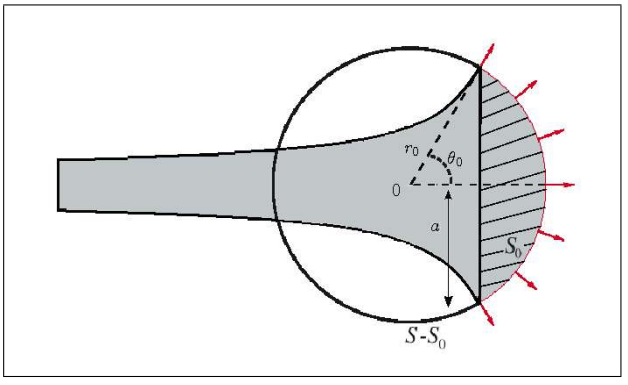

Figure 1. The radiation of the horn is approximated by that of a sphere S, part of which, S_0, is pulsating with a uniform velocity while the rest remains motionless. The radius of S is denoted r_0, the angle of the tangent cone at the horn output is denoted θ_0 and the radius of the end section of the horn is denoted a. From [8].

verify this model experimentally. This impedance is then averaged over S_0 in order to remove the dependence on spatial variables. The analytical expression includes an infinite sum, but can be simplified with a second order high-pass model,

$$Z_r(\omega) = Z_c \frac{\mathrm{i}\nu \dfrac{P_\nu}{P_\alpha} - \left(\nu P_\nu\right)^2}{1 + 2\mathrm{i}\nu P_\xi P_\nu - \left(\nu P_\nu\right)^2}, \qquad (4)$$

where $P_\alpha(\theta_0), P_\xi(\theta_0)$ and $P_\nu(\theta_0)$ are low order polynomials whose coefficients are given in Table I and $\nu = r_0 f/c$ is a non-dimensional variable.

Figure 2 shows the modulus of the reflection coefficient and the dimensionless length correction L/a of the plane and the spherical models for the trombone bell studied and presented in the next section ($\theta_0 = 1.26$ rad, $r_0 = 11.5$ cm and $a = 11$ cm). The two reflection coefficients have almost the same behaviour for frequencies below $ka = 2$ since they follow the same asymptotic requirement at low frequency. Then, they begin to differ. The spherical model actually gives higher values for the modulus of the reflection coefficient than the plane model, which might intuitively seem wrong since the aim of a horn is to improve the radiation at high frequency. Nevertheless, an explanation can be found in the fact that the spherical model is designed to produce a causal physical response. That is not the case for the plane model, which aims at better approximating the Levine and Schwinger formulation at high frequency than causal plane models. This plane radiation model can thus tend towards zero quicker than the spherical one. As for the length correction, an interpretation of the same kind can be given for the differences at high frequency. At low frequency, however, the plane model tends to the known dimensionless static length correction of the unflanged case which is equal to 0.6133. As for the spherical model, it tends to a slightly higher value between the static length correction of the flanged, which is equal to 0.8216, and the unflanged plane cases.

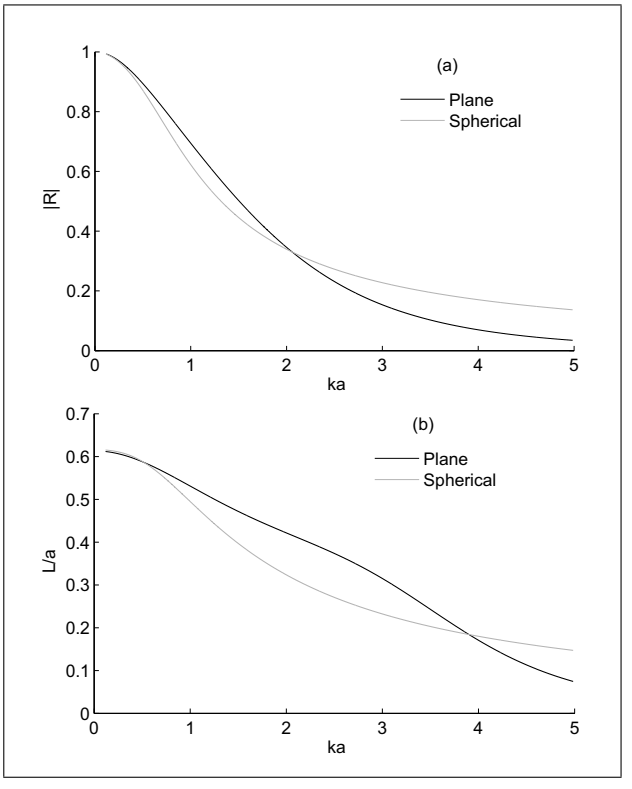

Figure 2. Modulus of (a) the reflection coefficient and (b) the dimensionless length correction L/a of the plane model (in black) and the spherical model (in grey) for the trombone bell.

Table I. Coefficients of the polynomials used in equation (4) which are functions of θ_0.

	θ_0^0	θ_0^1	θ_0^2
P_α	0.8788	1.0830	−1.24200
P_ξ	0.7200	0.0799	0.22100
P_ν	−0.0220	4.7040	−0.07946
	θ_0^3	θ_0^4	θ_0^5
P_α	1.1620	−0.6360	0.1113
P_ξ	−0.1440	0.0207	0.0000
P_ν	−0.4240	0.2607	−0.1980

2.3. Models including propagation and radiation

Two principal effects have to be taken into account so as to give a complete model of the horn: the wave propagation and the radiation. In order to evaluate the influence of each effect, four models constructed from the combination of the two wave propagation models from Section 2.1 and the two radiation impedances from Section 2.2 are compared (see Table II).

Two horns are studied in this paper. The first one is a tenor trombone bell which starts, following the slide section, with a cylindrical section of 10.4-mm radius. It begins to flare modestly, terminating in an abrupt flare to a radius of 110 mm after a 568-mm length (see Figure 3). The second one is a straight trumpet section of length 664.9 mm that begins with a long cylindrical part of 5.8-

Table II. The four models compared in this study. P stands for Plane and S for Spherical.

Model	1	2	3	4
Propagation	P	P	S	S
Radiation	P	S	P	S

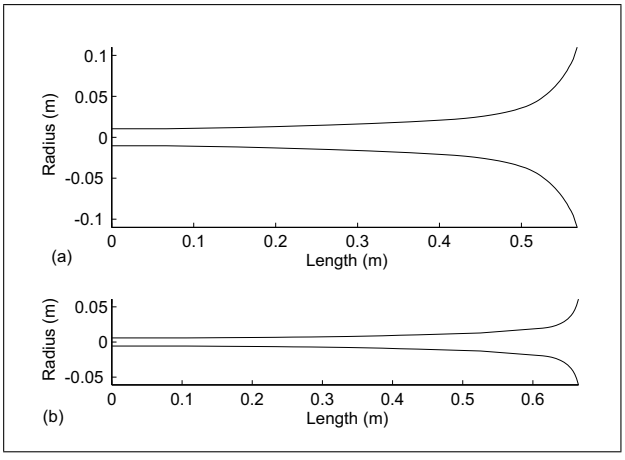

Figure 3. Geometry of (a) the trombone horn and (b) the trumpet horn.

mm radius and ends at a radius of 61.1 mm (see Figure 3). The mandrel of the trumpet horn was measured with an accuracy to within a hundreth of a millimetre and the geometry of the trombone was directly measured on the horn with an accuracy to within a tenth of a millimetre.

All results of these combinations are shown in Figure 4 for the trombone bell and in Figure 5 for the trumpet bell. These figures show that curves made from the same propagation model are close to each other in all frequency ranges. This means that the propagation model has a more important impact on the input impedance behaviour than the radiation model. Moreover, the spherical model realises a better impedance adaptation since, at high frequency, peaks are much lower for spherical than for plane propagation.

As the respective influence of both propagation and radiation models have been highlighted in this section, we choose for the rest of the article just to focus on two models: Model 1 and Model 4.

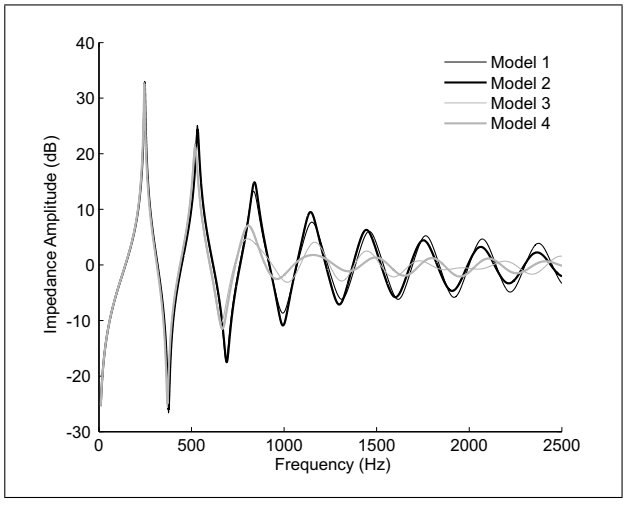

Figure 4. Comparison of the four proposed models of the trombone bell input impedance. Wave propagation: Plane (in black) and Spherical (in grey). Radiation: Plane (thin curves) and Spherical (thick curves).

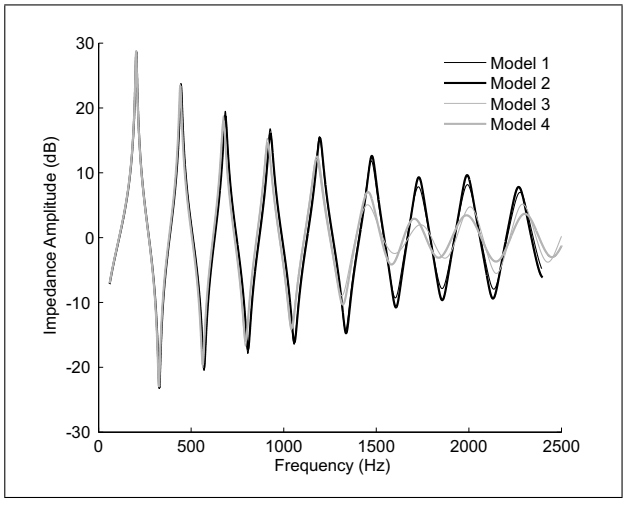

Figure 5. Comparison of the four proposed models of the trumpet bell input impedance. Wave propagation: Plane (in black) and Spherical (in grey). Radiation: Plane (thin curves) and Spherical (thick curves).

3. Experiment results and discussion

3.1. Experiment set-up

For the input impedance measurement, a set-up developed jointly by CTTM [30] and LAUM [31] is used [32]. In this apparatus, a small closed cavity in which a microphone measures a pressure p_1 (from which the volume velocity of the source is determined) is connected to the back of a piezo-electric buzzer. The measured pipe is connected to the front of the buzzer via a small open cavity in which a second microphone measures a pressure p_2. The input impedance is then calculated from the transfer function between the two microphones.

The source signal is a logarithmic chirp of five seconds length (generated by the PC audio sound card) leading to a frequency resolution of 0.2 Hz, from 50 to 2500 Hz. Finally, the measurement is obtained by averaging three acquisitions. The entire apparatus is placed in an anechoic chamber whose temperature has been estimated previously by measuring the input impedance of a closed cylinder of length 624 mm and radius 10.9 mm. According to Macaluso and Dalmont in [33], the measurement set-up allows the determination of the resonance frequencies with an uncertainty of about 0.2%. Moreover, this measurement apparatus was first tested by the authors with simple known cases, in particularly with the cylinder mentioned before. The difference between the measurement and the

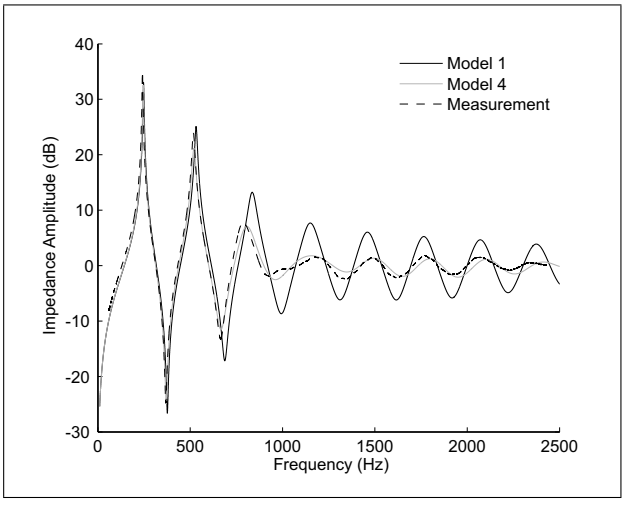

Figure 6. Comparison between the measurement of the trombone bell input impedance (dashed line) and the two models: the plane (in black) and the spherical (in grey).

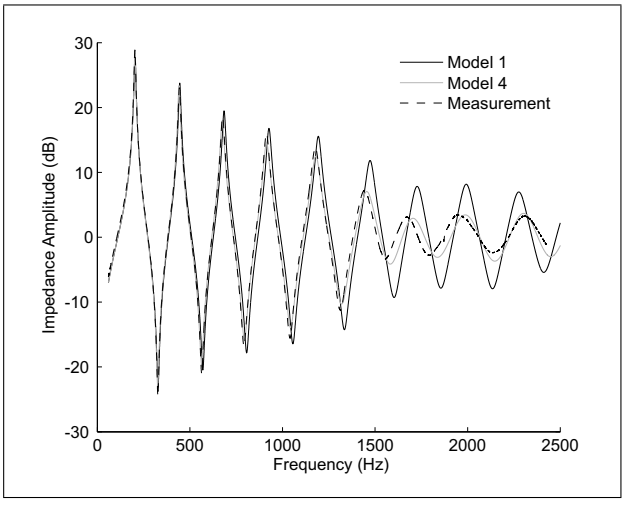

Figure 7. Comparison between the measurement of the trumpet bell input impedance (dashed line) and the two models: the plane (in black) and the spherical (in grey).

model (TMM with axial abscissa and radiation with a finite flange from [27]) in frequency was less than 0.15% for all resonance peaks. This uncertainty allows one to make a meaningful comparison between the different models and the measurements of the horns.

The input impedance of each of the two horns was measured six times, removing the bell from the impedance sensor each time in order to study the reproducibility. The reproducibility error is about 0.2%. Consequently, measurements of these horns can be considered as a reference for the comparison with the models. This comparison between models and measurement is shown in Figure 6 for the trombone bell and in Figure 7 for the trumpet bell.

3.2. Results

The behaviour of the curves in Figure 6 and 7 is different below and above the cutoff frequency F_c of the bell (see Benade [34]) which is around 700 Hz for the trombone and 1300 Hz for the trumpet. Below that frequency, the resonance peaks are sharp since the acoustic waves are reflected almost completely by the bell, whereas after, radiation is more important and the peaks decrease significantly in amplitude. When studying a musical instrument, it is interesting to look at its resonance characteristics, which are related to the playing frequencies. At high frequency there are no more resonances; for this reason it is more useful to examine the fluctuations of the reflection coefficient modulus above F_c.

Table III. Differences between the measured and modeled resonance peaks of the trombone horn at low frequency.

Resonance	Measurement	Model 1	Model 4
1st	Fr=241.43 Hz A=35.05 dB	2.7% 0.41 dB	1.8% -0.02 dB
2nd	Fr=517.22 Hz A=23.89 dB	2.8% 1.53 dB	0.6% -2.52 dB

Table IV. Differences between the measured and modeled resonance peaks of the trumpet horn at low frequency.

Resonance	Measurement	Model 1	Model 4
1st	Fr=202.87 Hz A=29.00 dB	0.83% 2.42 dB	0.56% 2.40 dB
2nd	Fr=443.09 Hz A=23.03 dB	0.52% 1.20 dB	-0.37% 0.77 dB
3rd	Fr=676.53 Hz A=18.59 dB	1.18% 1.04 dB	-0.27% -0.49 dB
4th	Fr=913.41 Hz A=16.00 dB	1.48% 0.84 dB	0.07% -1.38 dB
5th	Fr=1177.20 Hz A=13.83 dB	1.38% 1.80 dB	0.26% -1.27 dB

3.2.1. Low frequency analysis

Below the cutoff frequency, the models can be compared in terms of the impedance resonance peaks. These peaks are defined by three criteria: the frequency, the amplitude and the quality factor. In order to help craftsmen to design their musical instruments, the frequency criterion is the most important, as it is directly linked to the instrument tuning. The amplitude and quality factor have a small audible effect on the timbre and primarily affect the playing response. Here a comparison is done on the frequencies and amplitudes of the peaks, which are precisely determined with a peak fitting technique using a least square method (see Le Roux [35]).

The results in Tables III and IV show that the spherical model gives resonance frequencies closer to the measured values than the planar one. This supports the hypothesis of the quasi-sphericity of wavefronts which was experimentally established in the low frequency range by Benade and Jansson [16, 17]. The measured input impedance is expected to be located between the plane and the spherical models. This is actually the case for the second and

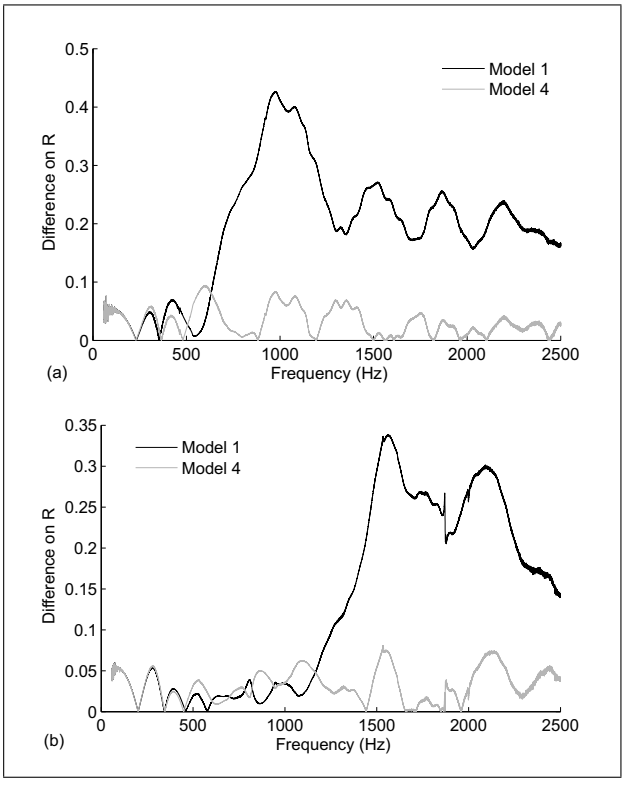

Figure 8. Modulus of the difference between the two proposed models (Plane model (in black) and Spherical model (in grey)) and the measurement on the reflection coefficient R (a) for the trombone and (b) for the trumpet.

third impedance peaks of the trumpet bell, with the measurement closer to the spherical model. The measured frequencies of the higher resonances, which are lower than predicted by both plane and spherical models, suggest that the radiation is even greater at these frequencies. No explanation can be given regarding why in both horns the measured frequency of the first resonance is lower than predicted by both models. Moreover it was checked in section 3.1 that there was no problem with the measurement apparatus.

3.2.2. High frequency analysis

Above the cutoff frequency, as the peaks do not have a sufficient sharpness, a good way to evaluate the accuracy of each model is to look at the reflection coefficient. Figure 8 shows the modulus of the difference between the reflection coefficient of each model and the measured one. In this figure, it clearly appears that the two models behave more similarly below the cutoff frequency than above. At low frequencies, the sound waves are not able to travel along the horn and as a result they are reflected. The reflection coefficient is thus approximately equal to one, regardless of the model used. At frequencies above the cutoff frequency, the bell becomes able to transmit waves to the lower end of the air column where they are reflected or radiated. Consequently, radiation has an important role in that frequency range. The spherical model (Model 4) has the closest fit to the measurements as the model of a pulsating portion of sphere realises a better impedance adaptation than the planar piston.

Table V. Differences between the spherical model and the measurement for the resonance peaks of the whole trombone.

Resonance	Measurement	Model 1	Model 4
2nd	Fr=111.80 Hz	1.50% (25.7 cents)	1.44% (24.8 cents)
	A=66.53 dB	1.95 dB	1.94 dB
3rd	Fr=170.09 Hz	1.46% (25.0 cents)	1.33% (22.9 cents)
	A=64.96 dB	1.56 dB	1.55 dB
4th	Fr=231.39 Hz	0.69% (11.9 cents)	0.49% (8.5 cents)
	A=64.72 dB	-0.08 dB	-0.13 dB
5th	Fr=299.27 Hz	0.18% (3.1 cents)	-0.04% (0.7 cents)
	A=68.21 dB	-0.76 dB	-0.94 dB
6th	Fr=353.12 Hz	0.33% (5.7 cents)	0.06% (1.0 cents)
	A=68.28 dB	-0.07 dB	-0.26 dB
7th	Fr=412.37 Hz	0.79% (13.6 cents)	0.32% (5.5 cents)
	A=62.47 dB	1.55 dB	0.91 dB
8th	Fr=471.53 Hz	0.59% (10.2 cents)	0.21% (3.7 cents)
	A=65.67 dB	0.90 dB	0.19 dB

4. An application for musical instruments craftsmanship: Extension to the whole trombone

In order to show the effective influence of the bell on a whole instrument, the remaining part of the trombone is added at the input end of the trombone horn, as shown in Figure 9. As it is impossible to measure the geometry of this remaining part with the same accuracy as for the trombone horn, only the plane propagation model is thus computed on this added part, taking the trombone horn input impedances calculated and measured in Section 3 as three different loads. By extending numerically the measurement of the trombone horn input impedance we thus create an "hybrid model". Results are shown in Figure 10, where the first "hybrid" resonance peak is not represented since it appears below 50 Hz and no measurement has been done below that frequency.

Table V suggests that the bell has a strong influence on the acoustics of the whole instrument. Indeed, even thought the horn only represents 20% of the trombone length, and the model of the additional part is exactly the same for the three curves in Figure 10, there is still a difference of more than 1% between the spherical model and the measurement for the second and third resonance frequencies. Nevertheless, the spherical model still gives an approximation of the resonance frequencies that is closer

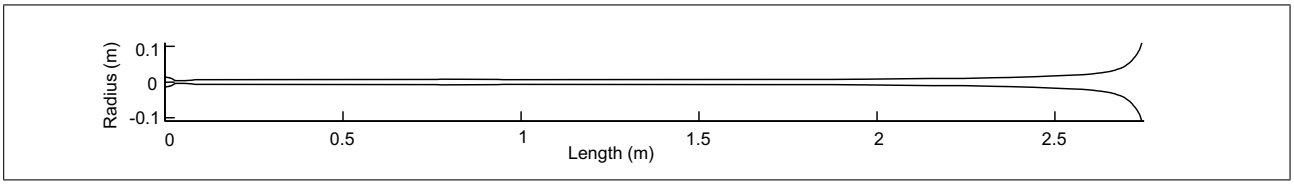

Figure 9. Geometry of the bell extended to the whole trombone.

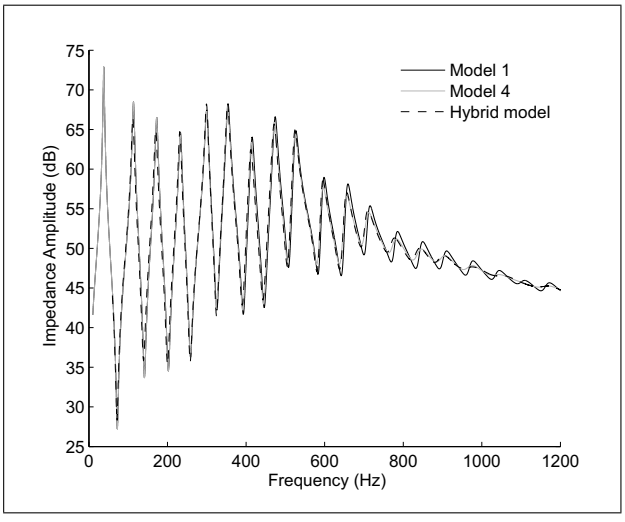

Figure 10. Input impedance of the bell virtually extended to the whole trombone: Comparison between the plane model (in black), the spherical model (in grey) and the hybrid model (dashed line).

to the measurement than the plane model, with a difference between the two models rising up to 8 cents for the seventh resonance. Moreover, it can be directly seen in Figure 10 that at high frequencies the spherical model follows the behaviour of the measurement well.

5. Conclusion

The comparison between two 1D models (a plane and a spherical) and the measurements of two brass instrument bells, allows assessment of both propagation and radiation models for a horn. Below the horn cutoff frequency, wave propagation predominates over radiation, since most of the waves are reflected by the horn. The spherical model (rather than the plane model) gives results closer to measurement for both horns, with the error in the predicted resonance frequencies less than 1% for all peaks (apart from the first one in the trombone). Above the cutoff frequency more waves are radiated and the comparison with measurement shows that the model of the pulsating portion of sphere is well adapted to the problem of horn modeling. This article has thus shown that the spherical 1D model approximates the acoustic behaviour of a horn more accurately than the plane 1D model. Nevertheless, this model still does not fit perfectly with the measurement.

The results might be then compared with other methods, such as Finite Element Methods, Boundary Elements Methods, Finite-Difference Time-Domain Methods, or Multimodal Methods. To this end, a benchmark test is currently in progress in order to compare all these methods with the measurements and models presented in this paper. This test is done on four different horns: the two horns studied in this article and two other cone-shaped horns. The first results of this work can be seen in [36].

In conclusion, for musical instrument craftsmanship applications, the 1D spherical model can be considered a good alternative to the currently used plane model, as differences between the model and the measurement do not rise above 25 cents (which is audible but still a substantial improvement). The model is particularly useful since it does not require very high computing power (any musical instrument maker should be able to use the designed software with his own personal computer) and calculations are fast.

Acknowledgments

This research was funded by the French National Research Agency ANR within the PAFI project (Plateforme d'Aide à la Facture Instrumentale in French). The authors would like to thank all participants, as well as T. Hélie from Ircam-CNRS, for all discussions and interesting work done together. Thank you also to P. Hoekje from Baldwin Wallace College for proofreading and valuable talks.

References

[1] J. Backus: Input impedance curves for the reed woodwind instruments. J. Acoust. Soc. Am. **56** (1974) 1266–1279.

[2] J. W. Coltman: Sounding mechanism of the flute and organ pipe. J. Acoust. Soc. Am. **43** (1968) 983–92.

[3] D. H. Lyons: Resonance frequencies of the recorder (english flute). J. Acoust. Soc. Am. **70** (1981) 1239–47.

[4] J.-P. Dalmont, B. Gazengel, J. Gilbert, J. Kergomard: Some aspects of tuning and clean intonation in reed instruments. App. Acoustics **46** (1995) 19–60.

[5] W. M. Hartmann: Pitch, periodicity, and auditory organization. J. Acoust. Soc. Am. **100** (1996) 3491–3502.

[6] G. R. Plitnik, W. J. Strong: Numerical method for calculating input impedances of the oboe. J. Acoust. Soc. Am **65** (1979) 816–825.

[7] M. van Walstijn, M. Campbell: Discrete-time modeling of woodwind instrument bores using wave variables. J. Acoust. Soc. Am. **113** (2003) 575–585.

[8] T. Hélie, X. Rodet: Radiation of a pulsating portion of a sphere: Application to horn radiation. Acta Acustica united with Acustica **89** (2003) 565–577.

[9] A. H. Benade: On woodwind instrument bores. J. Acoust. Soc. Am. **31** (1959) 137–146.

[10] N. Amir, V. Pagneux, J. Kergomard: A study of wave propagation in varying cross-section waveguides by modal decomposition. Part II: Results. J. Acoust. Soc. Am. **101** (1997) 2504–2517.

[11] J. A. Kemp, N. Amir, D. M. Campbell: Calculation of input impedance including higher modes. Proc. 5th French Congress on Acoustics, Lausanne, Switzerland, 2000, 314–317.

[12] J. A. Kemp, N. Amir, D. M. Campbell, M. van Walstijn: Multimodal propagation in acoustic horns. Proc. International Symposium on Musical Acoustics, Perugia, Italy, 2001, 521–524.

[13] A. Lefebvre: Computational acoustic methods for the design of woodwind instruments. Dissertation. Computational Acoustic Modeling Laboratory, McGill University, Montreal, Quebec, Canada, 2010.

[14] D. Noreland: A numerical method for acoustic waves in horns. Acta Acustica united with Acustica **88** (2002) 576–586.

[15] R. Caussé, J. Kergomard, X. Lurton: Input impedance of brass musical instruments - Comparison between experiment and numerical models. J. Acoust. Soc. Am. **75** (1984) 241–245.

[16] A. H. Benade, E. V. Jansson: On plane and spherical waves in horns with nonuniform flare. I. Theory of radiation, resonance frequencies, and mode conversion. Acustica **31** (1974) 79–98.

[17] E. V. Jansson, A. H. Benade: On plane and spherical waves in horns with nonuniform flare. II. Prediction and measurements of resonance frequencies and radiation losses. Acustica **31** (1974) 185–202.

[18] C. J. Nederveen, J.-P. Dalmont: Corrections to the plane-wave approximation in rapidly flaring horns. Acta Acustica united with Acustica **94** (2008) 471–473.

[19] J. Agulló, A. Barjau, D. H. Keefe: Acoustics propagation in flaring, axisymmetric horns: I. A new family of unidimensional solutions. Acustica united with Acta Acustica united with Acustica **85** (1999) 278–284.

[20] D. H. Keefe, A. Barjau: Acoustics propagation in flaring, axisymmetric horns: II. Numerical results, WKB theory, and viscothermal effects. Acta Acustica united with Acustica **85** (1999) 285–293.

[21] T. Hélie: Unidimensional models of acoustic propagation in axisymmetric waveguides. J. Acoust. Soc. Am. **114** (2003) 2633–2647.

[22] T. Hélie, T. Hézard, R. Mignot, D. Matignon: On the 1D wave propagation in wind instruments with a smooth profile. Proceedings of Forum Acusticum, Aalborg, Denmark, 2011, 521–526.

[23] H. Levine, J. Schwinger: On the radiation of sound from an unflanged circular pipe. Physical Review **73** (1948) 383–406.

[24] A. N. Norris, I. C. Sheng: Acoustic radiation from a circular pipe with an infinite flange. J. Sound Vib. **135** (1989) 85–93.

[25] F. Silva, P. Guillemain, J. Kergomard, B. Mallaroni, A. N. Norris: Approximation formulae for the acoustic radiation impedance of a cylindrical pipe. J. Sound Vib. **322** (2009) 255–263.

[26] W. E. Zorumski: Generalized radiation impedances and reflection coefficients of circular and annular ducts. J. Acoust. Soc. Am. **54** (1973) 1667–1673.

[27] J.-P. Dalmont, C. J. Nederveen, N. Joly: Radiation impedance of tubes with different flanges: numerical and experimental investigation. J. Sound Vib. **244** (2001) 505–534.

[28] P. M. Morse, K. U. Ingard: Theorical acoustics. McGraw-Hill, 1968, Ch. The Radiation of Sound, 332–356.

[29] M. Bruneau: Introduction aux théories de l'acoustique. Université du Maine, 1983, Ch. L'équation d'onde en coordonnées sphériques et cylindriques, 109–112.

[30] Centre de Transfert de Technologie du Mans, 20 rue Thales de Milet, 72000 Le Mans, France.

[31] Laboratoire d'Acoustique de l'Universite du Maine, UMR CNRS 6613, Avenue Olivier Messiaen, 72085 Le Mans Cedex 9, France.

[32] J.-P. Dalmont, J. C. Le Roux: A new impedance sensor for wind instruments. J. Acoust. Soc. Am. **123** (2008) 3014.

[33] C. A. Macaluso, J.-P. Dalmont: Trumpet with near-perfect harmonicity: design and acoustic results. J. Acoust. Soc. Am. **129** (2011) 404–414.

[34] A. H. Benade: Fundamental of musical acoustics. 1976, Ch. The Woodwinds: I, 430–464.

[35] J.-C. Le Roux: Le haut-parleur électrodynamique: estimation des paramètres électroacoustiques aux basses fréquences et modélisation de la suspension. Dissertation. Université du Maine, 1994.

[36] P. Eveno, J.-P. Dalmont, R. Caussé, J. Gilbert: Comparisons between models and measurements of the input impedance of brass instruments bells. Proceedings of Forum Acusticum 2011, Aalborg, Denmark, 567–572.